



Benthic O₂ uptake of two cold-water coral communities estimated with the non-invasive eddy correlation technique

Lorenzo Rovelli^{1,*}, Karl M. Attard^{2,3}, Lee D. Bryant^{4,8}, Sascha Flögel⁴,
Henrik Stahl^{1,9}, J. Murray Roberts^{1,5,6}, Peter Linke⁴, Ronnie N. Glud^{1,2,3,7}

¹Scottish Association for Marine Sciences, Scottish Marine Institute, Oban PA37 1QA, UK

²Nordic Centre for Earth Evolution (NordCEE), University of Southern Denmark, 5230 Odense M, Denmark

³Greenland Climate Research Centre, Greenland Institute of Natural Resources, 3900 Nuuk, Greenland

⁴GEOMAR, Helmholtz Centre for Ocean Research Kiel, 24148 Kiel, Germany

⁵Centre for Marine Biodiversity and Biotechnology, School of Life Sciences, Heriot-Watt University, Edinburgh EH14 4AS, UK

⁶Center for Marine Science, University of North Carolina Wilmington, Wilmington, NC 28409, USA

⁷Arctic Research Centre, University of Århus, 8000 Århus C, Denmark

⁸Present address: Department of Architecture and Civil Engineering, University of Bath, Bath BA2 7AY, UK

⁹Present address: Zayed University, Dubai Academic City, Dubai, United Arab Emirates

ABSTRACT: The community respiration of 2 tidally dominated cold-water coral (CWC) sites was estimated using the non-invasive eddy correlation (EC) technique. The first site, Mingulay Reef Complex, was a rock ridge located in the Sea of Hebrides off Scotland at a depth of 128 m and the second site, Stjærnsund, was a channel-like sound in Northern Norway at a depth of 220 m. Both sites were characterized by the presence of live mounds of the reef framework-forming scleractinian *Lophelia pertusa* and reef-associated fauna such as sponges, crustaceans and other corals. The measured O₂ uptake at the 2 sites varied between 5 and 46 mmol m⁻² d⁻¹, mainly depending on the ambient flow characteristics. The average uptake rate estimated from the ~24 h long deployments amounted to 27.8 ± 2.3 mmol m⁻² d⁻¹ at Mingulay and 24.8 ± 2.6 mmol m⁻² d⁻¹ at Stjærnsund (mean ± SE). These rates are 4 to 5 times higher than the global mean for soft sediment communities at comparable depths. The measurements document the importance of CWC communities for local and regional carbon cycling and demonstrate that the EC technique is a valuable tool for assessing rates of benthic O₂ uptake in such complex and dynamic settings.

KEY WORDS: Eddy correlation · Cold-water coral · Community oxygen exchange · Mingulay Reef Complex · Stjærnsund

INTRODUCTION

Cold-water corals (CWC) are azooxanthellate cnidarians that occur worldwide on continental shelves, slopes, seamounts and ridge systems. CWC may occur as individual polyps (such as the cup corals), as discrete colonies, such as the black corals (Anti-

patharia), or as reef framework-forming colonies such as the scleractinian *Lophelia pertusa*. The distribution may extend anywhere from small patches on the seabed to giant coral carbonate mounds of several kilometers in diameter (Roberts et al. 2006). The complex structural framework provides niches for a great biomass and diversity of organisms such as

*Corresponding author: lorenzo.rovelli@sams.ac.uk

© The authors 2015. Open Access under Creative Commons by Attribution Licence. Use, distribution and reproduction are unrestricted. Authors and original publication must be credited.

echinoderms, crustaceans, sponges and fish (Roberts & Cairns 2014). The communities trap large amounts of organic material and are thus considered to have the capability of turning over considerable amounts of organic material (van Oevelen et al. 2009, White et al. 2012). This has emphasized the need to further investigate CWC metabolism and to better quantify CWC community contributions to local and regional carbon budgets (Roberts et al. 2009).

However, the assessment of CWC reef community respiration rates poses major methodological challenges due to the structural complexity and spatial heterogeneity of the reefs. Traditional methods are invasive and rely on *ex situ* incubations of reef coral fragments (Dodds et al. 2007), *in situ* incubations of reef community sub-samples combined with complex food-web modeling (van Oevelen et al. 2009), and *in situ* benthic chamber deployments (Khripounoff et al. 2014). As per the current literature, the only non-invasive integrated estimates of CWC reef community respiration rates have been limited to open-water approaches that rely on benthic boundary layer (BBL) O_2 budget estimates from 2 or more coincident fixed-point O_2 measurements over the selected CWC reef area (White et al. 2012). The robustness of the O_2 budget as resolved using this approach strongly depends on how well the water-mass residence time within the target area is constrained spatially and temporally and, therefore, appears most suitable for channel-like sites.

The O_2 eddy correlation (EC) technique is a non-invasive *in situ* technique that is used to infer the benthic O_2 exchange rate from direct measurements of the turbulent transport of O_2 within the BBL (Berg et al. 2003). In homogenous, cohesive sediments deprived of conspicuous fauna, O_2 uptake rates derived from EC and benthic chambers, as well as from sediment–water microprofiling, are generally similar (e.g. Berg et al. 2003, 2009). Yet, one significant advantage of the EC technique is that it can be deployed on hard substrates, where chamber and microprofile measurements are easily compromised or fail entirely. The EC technique has been successfully applied to structurally complex, hard benthic substrates such as tropical coral reefs (Long et al. 2013), high-latitude rocky embayments (Glud et al. 2010) and oyster beds (Reidenbach et al. 2013). Since EC O_2 exchange measurements are obtained under natural hydrodynamics and characterize large areas of the seabed, the measurements integrate much of the site-specific spatial and temporal variability and provide a robust measure of benthic O_2 exchange of heterogeneous benthic

communities (Rheuban & Berg 2013). Here we present results of a study focused on applying the EC technique to assess the integrated community respiration of 2 CWC settings: (1) the Mingulay Reef Complex located in the Sea of Hebrides off Scotland and (2) the Stjærnsund located in northern Norway.

MATERIALS AND METHODS

Study sites

Mingulay Reef Complex. The Mingulay Reef Complex ($56^{\circ}47'N$, $7^{\circ}25'W$; Fig. 1a) is a 20 km long, 10 km wide, 70 to 250 m deep area located in the Sea of the Hebrides off Scotland and is characterized by the localized occurrence of CWC structures (Eden et al. 1971, Griffiths 2002, Roberts et al. 2005). The present study was performed at Mingulay Area 1 (see Roberts et al. 2009 and references therein) during the 'Changing Oceans' cruise, RRS 'James Cook' Cruise 073 (18 May–15 June 2012). The EC instrument (Fig. 1c) was placed on the seabed by the remotely operated vehicle (ROV) Holland-1 (see www.marine.ie/Home/site-area/infrastructure-facilities/research-vessels/deepwater-rov) at a depth of 128 m. Small coral mounds of live *Lophelia pertusa* as well as crinoids *Leptometra* sp. and sponges were present in the vicinity of the instrument (Fig. 1e). The flow velocity at the seabed was tidally driven and ranged from 5 to 33 $cm\ s^{-1}$ (average $13.5 \pm 4.5\ cm\ s^{-1}$).

Stjærnsund reef. Stjærnsund ($70^{\circ}30'N$, $22^{\circ}30'E$; Fig. 1b) is a 30 km long, 3.5 km wide, >400 m deep glacial sound in northern Norway that connects the Altafjord to North Atlantic waters (Rüggeberg et al. 2011). A submerged SW-NE morainic sill in the area hosts one of Europe's northernmost CWC reefs (Dons 1932, Freiwald et al. 1997). The crest of the sill was dominated by a sponge-hydroid community, mainly *Mycale* sp. and *Tubularia* sp., and smaller patches of living *L. pertusa* (Fig. 1f). The present study targeted the sill crest, at a depth of 220 m, as part of a large modular multidisciplinary seafloor observatory (Molab) deployment. The Molab EC modules (ECMs; Fig. 1d) were deployed by the ROV Phoca (see www.geomar.de/en/centre/central-facilities/tlz/rovphoca/overview/) during the RV 'Poseidon' POS434 cruise (26 May–15 June 2012) and retrieved 4 mo later during the RV 'Poseidon' POS438 cruise (10–27 September 2012). The flow velocity at the seabed was tidally driven and ranged from 1 to 14 $cm\ s^{-1}$ (average $5.9 \pm 3.8\ cm\ s^{-1}$).

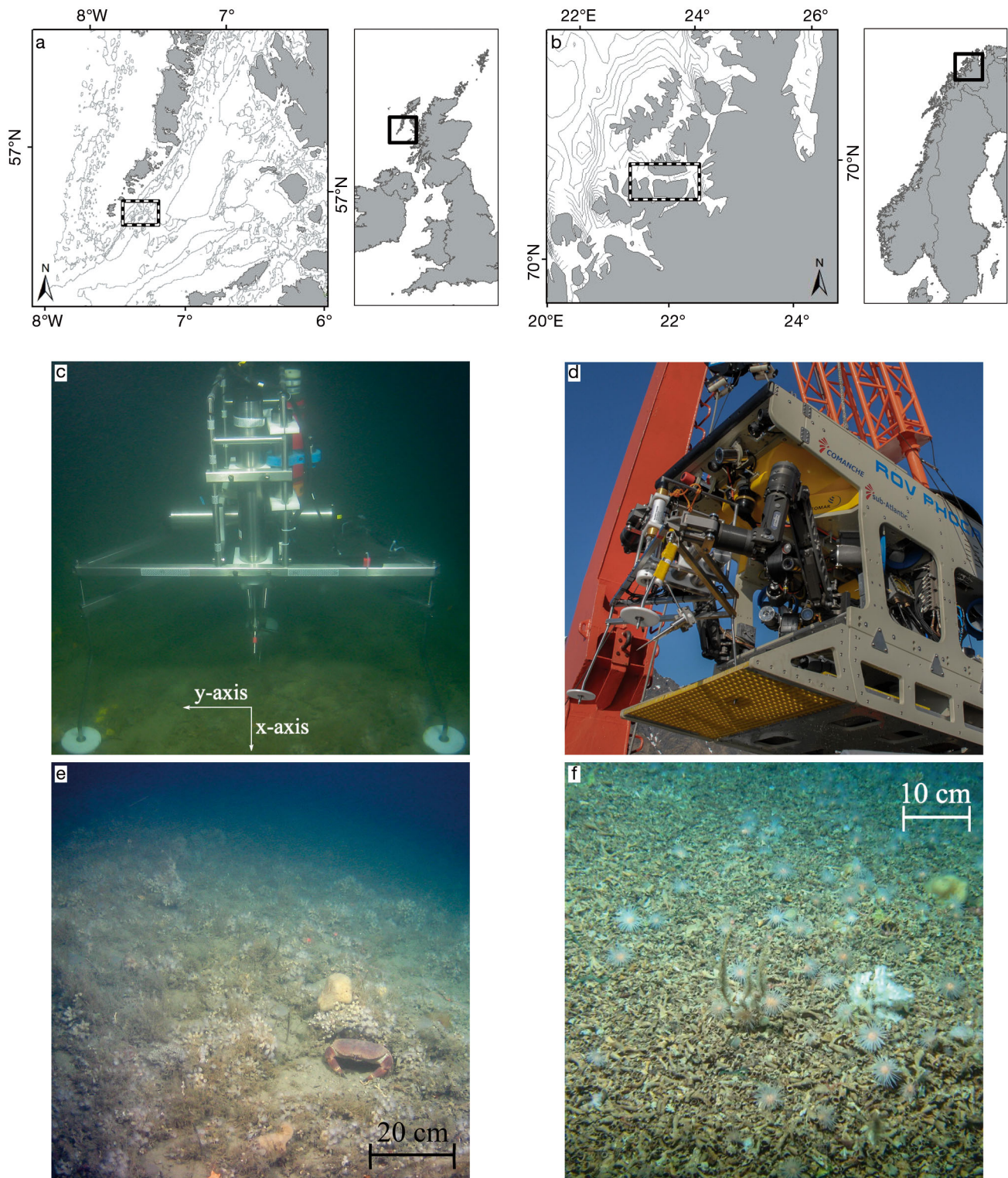


Fig. 1. Cold-water coral (CWC) sites and eddy correlation module (ECM) system deployments. Location of (a) the Mingulay Reef Complex and (b) the Stjærnsund site. ECM deployed at (c) Mingulay and (d) on the ROV Phoca during deployment at the Stjærnsund (photo by P. Linke). Overview of the eddy correlation (EC) footprint area at (e) Mingulay and (f) Stjærnsund, respectively. Underwater images for Mingulay and the Stjærnsund are courtesy of the ROV Holland-1 and Phoca teams, respectively

Eddy correlation measurements

Site selection. Before ECM deployment, ROV surveys were performed in the target areas to identify suitable spots for EC measurements. The main criteria for site selection were: (1) the presence of a flat area to safely deploy the frame, (2) a sufficient distance from large meter-sized structures and features (i.e. reef mounds and dense CWC patches) and (3) a representative CWC benthic community. Further emphasis was given to the ECM frame orientation with respect to the local flow hydrodynamics, aiming to both deploy the ECM in line with the main flow direction and avoid flow disturbances due to large structures in the vicinity of the ECMs. The ROV video footage was also used to describe the benthic community, i.e. the main taxa occurrence at each site.

Instrumental setup. The O_2 uptake estimations were performed with 2 ECMs, one from SDU (University of Southern Denmark; Mingulay site) and one from GEOMAR (Stjærnsund site). The setup of the ECMs was similar to the original design by Berg et al. (2003). The main components of the ECMs consisted of an acoustic Doppler velocimeter (ADV; Vector, Nortek) and Clark-type O_2 microelectrodes (Revsbech 1989) that relayed the signal to the ADV via submersible amplifiers (McGinnis et al. 2011). The O_2 electrodes had 90 % response times of 0.5 s while the stirring sensitivity was below 0.5 % (Gundersen et al. 1998). The ADV recorded the velocity components as well as the O_2 microsensor signals at a frequency of 64 Hz and, in addition, collected ancillary information such as the sampling distance from the seabed, flow direction, and signal strength. Each ECM was mounted onto a small stainless steel tripod frame that was designed specifically for deployment by ROV (McGinnis et al. 2011). A small conductivity-temperature-depth (CTD) logger equipped with an O_2 Aanderaa optode was mounted onto each ECM to collect background environmental information and for *in situ* calibration of the O_2 electrodes.

The ADV was mounted downward-facing perpendicular to the seabed surface, and the ADV sampling volume was located 25 and 13.5 cm above the seabed for the Mingulay Reef and Stjærnsund Reef deployments, respectively. The O_2 electrode tips were accurately placed very close (<1 cm) to the sampling volume, to ensure robust velocity- O_2 cross-correlations also during periods of flow perpendicular to the O_2 electrode orientation (Donis et al. 2014).

At the Mingulay Reef site, EC deployment was performed over 25 h. For the 4 mo deployment at Stjærnsund Reef, a timer was added to the ADV to control

the instrument's on-off times and thus increase battery duration in order to obtain periods of recording over the whole deployment time. The ECM timer was programmed to collect datasets every week. However, due to issues with the internal ADV logger, only one dataset of 22.5 h was recorded during the 4 mo measurement period.

Data processing. The ADV 64 Hz datasets were averaged down to 8 Hz for further processing. Quality controls included flagging ADV velocity data with beam correlations <50 % and signal-to-noise ratios (SNR) <10, as well as subsequent despiking of the O_2 and velocity time series (Matlab despiking toolbox; Goring & Nikora 2002). A planar-fit coordinate rotation was performed on the 8 Hz velocity data to obtain a vertical velocity component normal to the local streamline (Lorke et al. 2013).

The time-averaged turbulent O_2 flux (F_{O_2}) was estimated from vertical velocity fluctuations (w') and O_2 concentration fluctuations (C') as $F_{O_2} = \overline{w'C'}$ (Berg et al. 2003). The fluctuations were obtained via linear detrending based on Reynolds decomposition as $w' = w - \bar{w}$ and $C' = C - \bar{C}$ with w and C being the measured vertical velocities and O_2 concentrations, respectively, and \bar{w} and \bar{C} the time-averaged values. Data averaging, time shifting and O_2 flux estimates were performed using the Fortran program suite Sulfide-Oxygen-Heat Flux Eddy Analysis version 2.0 (www.dfmccginnis.com/SOHFEA; McGinnis et al. 2011). The window size (time interval) for the estimation of the turbulent fluctuations was inferred from the bulk averages over incrementally increased window sizes for O_2 fluxes (McGinnis et al. 2008, Attard et al. 2014) and shear velocity (u_* ; McPhee 2008). For both sites, a window size of 3 min was found to be an optimal trade-off between including the major turbulent contributions while minimizing the inclusion of non-turbulent processes; the resulting O_2 fluxes were subsequently averaged to 1 h intervals and presented as O_2 uptake rates, i.e. with positive values for O_2 fluxes directed from the water column towards the sediment.

The representative u_* averages for each window size were computed from Reynolds stress as:

$$u_* = \sqrt{-\overline{u'w'}} \quad (1)$$

with u' representing longitudinal flow fluctuations (Reidenbach et al. 2006, Inoue et al. 2011). The sediment surface roughness parameter (z_0) was estimated assuming logarithmic law-of-the-wall scaling as:

$$z_0 = z \cdot \exp\left(-\kappa \cdot \frac{U}{u_*}\right) \quad (2)$$

where z is the measurement height above the benthic surface, κ is the von Karman constant (0.41), and

U is the flow-velocity magnitude (Wüest & Lorke 2003). Mean z_0 was subsequently used to estimate the characteristics of the EC flux footprint from empirical relations that evaluate the downstream transport and dispersion of a dissolved conservative tracer at the seabed; the footprint area is defined as the smallest area of the seabed that contributes to 90 % of the measured flux (Berg et al. 2007).

Quality refinement of O_2 uptake rates encompassed: (1) removal of spikes due to sensor collisions with particles and debris, (2) flagging of measurements during abrupt flow direction changes and (3) exclusion of EC fluxes during periods of high anisotropy levels. The latter is based on the ratio between the average horizontal (ϵ_y) and vertical (ϵ_z) turbulent kinetic energy dissipation rates that were estimated from the ADV velocity time series using the inertial dissipation method (Inoue et al. 2011). A ratio of 1 implies full isotropy, i.e. well-developed turbulence in all directions, with increasing anisotropy the larger the ratio, i.e. the stronger the directional component in the turbulence. The threshold anisotropy used to constrain EC-favorable, near-isotropic conditions is dependent on the local hydrodynamics and topography; ratios of 12 and 9 were found to be most suitable for the settings at Mingulay and Stjernsund, respectively.

RESULTS

The EC deployment lasted 25 h at Mingulay. During the observational period, the average temperature was 9.30 ± 0.01 °C (mean \pm SD) and the O_2 concentration also showed minimal variation (245.8 ± 0.004 $\mu\text{mol l}^{-1}$, 88 % saturation). A semi-diurnal trend was clearly observed in the ADV hydrostatic pressure dataset (Fig. 2a). Although large hourly flow variability suggested a complex hydrodynamic regime, 2 main tidal current directions at 77° and -89° from the ADV x-velocity axis (i.e. the frame main orientation; Fig. 1c), were detected for flood and ebb tide respectively. The flood tide direction encompassed 47 % of the screened dataset and resulted in an O_2 uptake rate of 26.1 ± 3.1 $\text{mmol m}^{-2} \text{d}^{-1}$ ($n = 9$), while the rate for the opposite direction (ebb tide) was 26.4 ± 4.3 $\text{mmol m}^{-2} \text{d}^{-1}$ ($n = 10$). This suggested no directional uptake rate dependencies and relatively homogenous benthic environments on either side of the EC system, and was also confirmed visually from the ROV video surveys. The overall deployment average O_2 uptake was 27.8 ± 2.3 $\text{mmol m}^{-2} \text{d}^{-1}$ (mean \pm SE; Fig. 2e) ranging from 14.6 to 46.3 $\text{mmol m}^{-2} \text{d}^{-1}$. Shear

velocity based estimates of bottom roughness revealed a rough seabed topography with an average z_0 of 3.4 cm.

At the Stjernsund reef, the ECM collected 22.5 h of consecutive data. During the measurements, O_2 concentration ranged from 251 to 261 $\mu\text{mol l}^{-1}$ (average 255 ± 2.6 $\mu\text{mol l}^{-1}$), with near-constant temperature conditions (6.10 ± 0.02 °C). Semi-diurnal tidal signatures were observed in the hydrostatic pressure and flow regime (Fig. 2f,h), as well as in O_2 concentration (Fig. 2g), indicating a well-established tidal front moving along the Stjernsund channel. The most consistent O_2 uptake rates were obtained during periods of flood tide (Fig. 2f,j). In these periods, the O_2 concentrations remained constant (259 $\mu\text{mol l}^{-1}$; 86.5 % saturation), and the hourly O_2 uptake rates ranged from 4.8 to 40.8 $\text{mmol m}^{-2} \text{d}^{-1}$. During ebb tide, perturbed flow conditions due to the presence of a large coral mound resulted in a systematical flagging of the O_2 uptake rates, and thus the data collected during the ebb tide period were excluded from further analyses. The Stjernsund average O_2 uptake (flood tide only) was 24.8 ± 2.6 $\text{mmol m}^{-2} \text{d}^{-1}$ (mean \pm SE) while the average z_0 was 3.0 cm.

At both sites, the ROV video footage resolution was inadequate or impeded by poor visibility to infer detailed quantitative information about the abundance of the benthic fauna within the ECM vicinity and footprint areas. Nevertheless, we were able to describe the occurrence of large structures and dominant species. At Mingulay, the deployment area was characterized by fragments and rubble of dead corals. The latter were frequently colonized by the zooanthid *Parazoanthus anguicomus*, the sponge *Spongosorites coralliophaga* with a prominent coverage of hydroids, and suspension-feeding sabellid polychaetes. Occasional mobile invertebrates, notably the edible crab *Cancer pagurus*, were seen in the area. With the exception of the sparse living *L. pertusa* colonies, no substantial community difference was observed along the main tidal directions (Fig. 1e). The Stjernsund EC deployment area revealed sparse red and white gorgonians (*Paragorgia arborea*) intercalated with *Mycale lingua* sponges. Sea anemones, such as *Protanthea simplex*, and hydroids, such as *Tubularia indivisa*, covered the underlying coral rubble (Fig. 1f). Live orange *L. pertusa* mounds were mainly present on the side of the ECM frame outside the footprint. These structures, together with the gorgonians, represented the tallest features with a height of up to 50 cm and were responsible for the evident flow disruption during ebb tide.

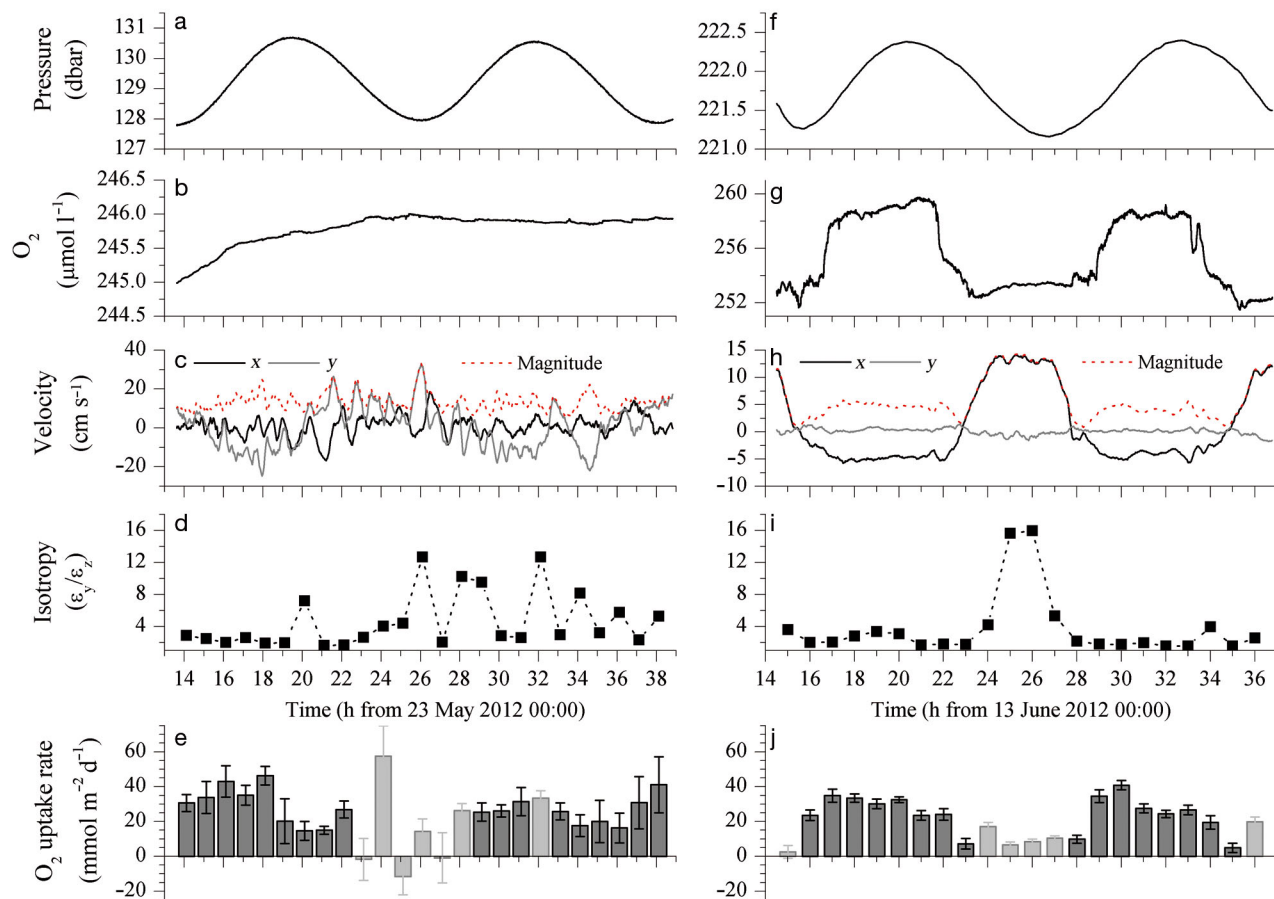


Fig. 2. EC datasets from (a–e) Mingulay and (f–j) the Stjærnsund CWC sites showing (a,f) hydrostatic pressure, (b,g) bulk water O_2 concentration from CTD optodes and (c,h) flow velocities along the acoustic Doppler velocimeter (ADV) x-axis (parallel to the frame orientation; black lines) and y-axis (perpendicular to the frame orientation; gray lines). Negative values indicate movements towards the ADV. Red dotted lines indicate current velocity magnitude. (d,i) Isotropic level, defined as the ratio between the horizontal (ϵ_z) and vertical (ϵ_x) turbulence level estimated using the inertial dissipation method. (e,j) Mean (\pm SE) turbulent O_2 uptake rates over 1 h intervals. Light gray bars indicate fluxes that were flagged due to high isotropic level, O_2 electrode collisions, abrupt flow direction changes and flow disruptions. Positive values indicate O_2 flux from the water column toward the sediment as opposed to negative values for O_2 flux directed away from the sediment. Note that the time, in hours, refers to the time elapsed starting from midnight of the deployment day (e.g. 24 represents midnight)

DISCUSSION

We were able to derive robust *in situ* estimates of the benthic O_2 uptake rate at 2 different CWC reef sites using the EC method. Despite the geographic separation and the differences in benthic communities, average O_2 uptake rates for Mingulay ($27.8 \text{ mmol } O_2 \text{ m}^{-2} \text{ d}^{-1}$) and Stjærnsund ($24.8 \text{ mmol } O_2 \text{ m}^{-2} \text{ d}^{-1}$) were similar. These rates are framed by the few available CWC literature values derived from incubations, which range from $7.7 \text{ mmol } O_2 \text{ m}^{-2} \text{ d}^{-1}$ for isolated *Lophelia pertusa* fragments (Khripounoff et al. 2014) to $74.5 \text{ mmol } O_2 \text{ m}^{-2} \text{ d}^{-1}$ for an entire CWC community (van Oevelen et al. 2009;

using a Redfield O_2 :C ratio of 138:106). Values from the open-water approach amount to 10.3 to $88 \text{ mmol } O_2 \text{ m}^{-2} \text{ d}^{-1}$ (White et al. 2012). The reported O_2 uptake rates are 4 to 5 times higher than the global average total benthic O_2 uptake rate (TOU) for soft sediments from comparable depths (7.8 and $5.2 \text{ mmol } O_2 \text{ m}^{-2} \text{ d}^{-1}$ for Mingulay and Stjærnsund, respectively) as derived from benthic chamber incubations (Glud 2008). Similarly, those values were ~ 4 times higher than *in situ* benthic O_2 uptake rates derived from microprofile measurements in soft muddy sediments at 329 m depth in Van Mijen Fjord ($69^\circ 29.4' \text{ N}$, $18^\circ 7.5' \text{ W}$; Glud et al. 1998), near Stjærnsund.

EC O₂ uptake rates are extracted under naturally varying *in situ* conditions and integrate a large footprint area. As such, they provide an integrative assessment of community respiration including faunal respiration and microbial-driven mineralization. The extent to which O₂ sinks on the reef are correctly integrated by the EC measurements depends on the characteristics of the EC flux footprint that is defined by the EC sensor measurement height and the local z_0 .

Due to the natural structural complexity of CWC, we observed z_0 values (3.4 and 3.0 cm for Mingulay and Stjærnsund, respectively) that were much higher than those typical for rough gravel or cobble beds (<0.5 cm; Reidenbach et al. 2010) and comparable to that of oyster beds (2.7 cm; Reidenbach et al. 2013). As increased z_0 results in increased turbulent mixing, the estimated footprint areas in the present study were relatively small. At Mingulay, the EC O₂ uptake integrated a footprint length of 11.8 m and width of 1.6 m (~15 m²) with the region of maximum flux about 0.1 m from the ADV. In comparison, the Stjærnsund footprint had a length of 3.5 m and a width of 0.9 m (2 to 3 m²) with the region of maximum flux located at the position of the sampling volume.

ROV inspection of the respective footprints showed that the majority of the footprint was homogeneously covered with coral rubble and associated small fauna such as zooanthids, sponges, anemones and hydroids (up to 10 × 10 cm in size). Based on the idealized patches model by Rheuban & Berg (2013) and the EC settings of this study, we inferred that our measurements integrated, within a 10% error, patch sizes of up to 50 × 50 cm at the Mingulay site and up to 20 × 20 cm at the Stjærnsund site, validating the inclusion of smaller fauna in our assessments.

The footage analysis also revealed the occurrence of larger isolated *L. pertusa* mounds (Fig. 1). At Mingulay, those features were only up to 20 cm tall, thus shorter or comparable with the EC measuring height and therefore well integrated into the EC measurements. At the Stjærnsund, however, some of the *L. pertusa* mounds extended above the EC measuring height and thereby their contribution to the overall community respiration may only have been partly included. The few studies on the relative contributions of *L. pertusa* respiration to total CWC reef community metabolism (e.g. van Oevelen et al. 2009) suggest that, due to their relatively low abundance, live *L. pertusa* mounds do not significantly contribute to total reef metabolism. Coupled modelling and *ex situ* incubations from the 800 m deep northeast Atlantic Rockall Bank suggested that *L. pertusa* only

contributed 9% of the total CWC reef community O₂ consumption (van Oevelen et al. 2009). Similarly, *in situ* incubations of *L. pertusa* fragments at the Brittany continental slope showed that they were responsible for an O₂ consumption rate of only ~8 mmol m⁻² d⁻¹ (Khripounoff et al. 2014). Considering that the coral mounds located within the EC footprints were fewer than in these studies above, it is reasonable to assume that full integration of their contributions would only result in a marginal increase of the EC-derived O₂ uptake.

Despite considerable logistic challenges, we documented that the EC method can be used to derive benthic O₂ exchange rates from different CWC reefs with complex topography and subsequently integrate O₂ uptake over relatively large areas of the seabed under unobstructed environmental conditions. The EC measurements integrate the activity of the entire benthic community provided that careful consideration is given to deployment planning. To ensure the inclusion of the extensive topographic features of CWC reefs, future studies should ideally be performed at a measurement height of 1.5 times the height of the main features observed (see Burba 2013). Future studies will allow *in situ* quantification of CWC responses to seasonally important environmental drivers such as temperature, flow and sedimentation so that ultimately the overall importance of CWC for regional and global carbon cycling can be assessed.

Acknowledgements. We are grateful to the crews of the RRS 'James Cook' and RV 'Poseidon' for their assistance throughout the respective research cruises. We thank A. Glud for providing the O₂ electrodes used in this study and A. Lorke for the Matlab ID script. We thank R. Schwarz and S. Cherednichenko of GEOMAR's Technology and Logistic center for their support during designing and building of the ECM frame, the amplifiers and the timer module as well as during the preparation and programming at sea. Furthermore, we thank the Holland-1 and Phoca ROV teams for safe deployment and recovery at the Mingulay and Stjærnsund sites, respectively. Funding for the Mingulay deployment was provided through the UK Ocean Acidification programme (NERC grant NE/H017305/1 and added-value awards to J.M.R.). Funding for Molab was provided by the Federal Ministry of Education and Research (BMBF) under grant 03F06241; the Poseidon cruises POS434 and POS438 were supported by GEOMAR and industry funding (grant A2300414 to P.L.). L.R., K.M.A. and R.N.G., received financial support from National Environmental Research Council (NERC) – NE/F018614/1, NE/J011681/1, NE/F0122991/1; The Commission for Scientific Research in Greenland (KVUG) – GCRC6507; The Danish Council for Independent Research (FNU-12-125843); ERC Advanced Grant, ERC-2010-AdG_20100224 and The Danish National Research Foundation (DRNF53). We are grateful to M. H. Long and 2 anonymous reviewers for comments that improved the manuscript.

LITERATURE CITED

- Attard KM, Glud RN, McGinnis DF, Rysgaard S (2014) Seasonal rates of benthic primary production in a Greenland fjord measured by aquatic eddy-correlation. *Limnol Oceanogr* 59:1555–1569
- Berg P, Røy H, Janssen F, Meyer V, Jørgensen BB, Huettel M, de Beer D (2003) Oxygen uptake by aquatic sediments measured with a novel non-invasive eddy-correlation technique. *Mar Ecol Prog Ser* 261:75–83
- Berg P, Røy H, Wiberg PL (2007) Eddy correlation flux measurements: the sediment surface area that contributes to the flux. *Limnol Oceanogr* 52:1672–1684
- Berg P, Glud RN, Hume A, Stahl H, Oguri K, Meyer V, Kitazato H (2009) Eddy correlation measurements of oxygen uptake in deep ocean sediments. *Limnol Oceanogr Methods* 7:576–584
- Burba G (2013) Eddy Covariance Method. Li-COR Biogeosciences, Lincoln, NE
- Dodds LA, Roberts JM, Taylor AC, Marubini F (2007) Metabolic tolerance of the cold-water coral *Lophelia pertusa* (Scleractinia) to temperature and dissolved oxygen change. *J Exp Mar Biol Ecol* 349:205–214
- Donis D, Holtappels M, Noss C, Cathalot C and others (2014) An assessment of the precision and confidence of aquatic eddy correlation measurements. *J Atmos Ocean Technol* 32:642–655
- Dons C (1932) Zoologiske Notiser XV. Om Nord-Norges korallsamfund. *K Nor Vidensk Selsk Forh* 5:13–16
- Eden RA, Arduin DA, Binns PE, McQuillin R, Wilson JB (1971) Geological investigations with a manned submersible off the west coast of Scotland 1969–1970. *Inst Geol Sci Rep* 71/16, H. M. Stationary Office, London
- Freiwald A, Henrich R, Pätzold J (1997) Anatomy of a deep-water coral reef mound from Stjernsund, West Finnmark, northern Norway. *SEPM (Soc Sediment Geol) Spec Publ* 56:141–161
- Glud RN (2008) Oxygen dynamics in marine sediments. *Mar Biol Res* 4:243–289
- Glud RN, Holby O, Hoffmann F, Canfield DE (1998) Benthic mineralization and exchange in Arctic sediments (Svalbard, Norway). *Mar Ecol Prog Ser* 173:237–251
- Glud RN, Berg P, Hume A, Batty P, Blicher ME, Lennert K, Rysgaard S (2010) Benthic O₂ exchange across hard-bottom substrates quantified by eddy correlation in a sub-Arctic fjord. *Mar Ecol Prog Ser* 417:1–12
- Goring DG, Nikora VI (2002) Despiking acoustic doppler velocimeter data. *J Hydraul Eng* 128:117–126
- Griffiths C (2002) Discovery 257. SAMS Northern Seas Programme, 21 Sep to 9 Oct 2001. Clyde-Clyde, Internal Cruise Report. Scottish Association for Marine Science, Oban
- Gundersen JK, Ramsing NB, Glud RN (1998) Predicting the signal of O₂ microsensors from physical dimensions, temperature, salinity, and O₂ concentration. *Limnol Oceanogr* 43:1932–1937
- Inoue T, Glud RN, Stahl H, Hume A (2011) Comparison of three different methods for assessing *in situ* friction velocity: a case study from Loch Etive, Scotland. *Limnol Oceanogr Methods* 9:275–287
- Khripounoff A, Caprais JC, Le Bruchec J, Rodier P, Noel P, Cathalot C (2014) Deep cold-water coral ecosystems in the Brittany submarine canyons (Northeast Atlantic): hydrodynamics, particle supply, respiration, and carbon cycling. *Limnol Oceanogr* 59:87–98
- Long MH, Berg P, de Beer D, Ziemann JC (2013) *In situ* coral reef oxygen metabolism: an eddy correlation study. *PLoS ONE* 8:e58581
- Lorke A, McGinnis DF, Maeck A (2013) Eddy-correlation measurements of benthic fluxes under complex flow conditions: effects of coordinate transformations and averaging time scales. *Limnol Oceanogr Methods* 11:425–437
- McGinnis DF, Berg P, Brand A, Lorrai C, Edmonds TJ, Wuest A (2008) Measurements of eddy correlation oxygen fluxes in shallow freshwaters: towards routine applications and analysis. *Geophys Res Lett* 35:L04403, doi: 10.1029/2007GL032747
- McGinnis DF, Cherednichenko S, Sommer S, Berg P and others (2011) Simple, robust eddy correlation amplifier for aquatic dissolved oxygen and hydrogen sulfide flux measurements. *Limnol Oceanogr Methods* 9:340–347
- McPhee M (2008) Air–ice–ocean interaction: turbulent ocean boundary layer exchange processes. Springer, Berlin
- Reidenbach MA, Monismith SG, Koseff JR, Yahel G, Genin A (2006) Boundary layer turbulence and flow structure over a fringing coral reef. *Limnol Oceanogr* 51:1956–1968
- Reidenbach MA, Limm M, Hondzo M, Stacey MT (2010) Effects of bed roughness on boundary layer mixing and mass flux across the sediment-water interface. *Water Resour Res* 46:W07530, doi:10.1029/2009wr008248
- Reidenbach MA, Berg P, Hume A, Hansen JCR, Whitman ER (2013) Hydrodynamics of intertidal oyster reefs: the influence of boundary layer flow processes on sediment and oxygen exchange. *Limnol Oceanogr Fluids Environ* 3:225–239
- Revsbech NP (1989) An oxygen microelectrode with a guard cathode. *Limnol Oceanogr* 34:474–478
- Rheuban J, Berg P (2013) The effect of benthic surface heterogeneity on eddy correlation flux measurements. *Limnol Oceanogr Methods* 11:351–359
- Roberts JM, Cairns SD (2014) Cold-water corals in a changing ocean. *Curr Opin Environ Sustain* 7:118–126
- Roberts JM, Brown CJ, Long D, Bates CR (2005) Acoustic mapping using a multibeam echosounder reveals cold-water coral reefs and surrounding habitats. *Coral Reefs* 24:654–669
- Roberts JM, Wheeler AJ, Freiwald A (2006) Reefs of the deep: the biology and geology of cold-water ecosystems. *Science* 312:543–547
- Roberts JM, Davies AJ, Henry LA, Dodds LA and others (2009) Mingulay reef complex: an interdisciplinary study of cold-water coral habitat, hydrography and biodiversity. *Mar Ecol Prog Ser* 397:139–151
- Rüggeberg A, Flögel S, Dullo WC, Hissmann K, Freiwald A (2011) Water mass characteristics and sill dynamics in a subpolar cold-water coral reef setting at Stjernsund, northern Norway. *Mar Geol* 282:5–12
- van Oevelen D, Duineveld G, Lavaleye M (2009) The cold-water coral community as a hot spot for carbon cycling on continental margins: a food-web analysis from Rockall Bank (northeast Atlantic). *Limnol Oceanogr* 54:1829–1844
- White M, Wolff GA, Lundalv T, Guihen D, Kiriakoulakis K, Lavaleye M, Duineveld G (2012) Cold-water coral ecosystem (Tisler Reef, Norwegian Shelf) may be a hotspot for carbon cycling. *Mar Ecol Prog Ser* 465:11–23
- Wüest A, Lorke A (2003) Small-scale hydrodynamics in lakes. *Annu Rev Fluid Mech* 35:373–412